SINET: *Ethiop. J. Sci.*, 39(2):108-115, 2016 ISSN: 0379–2897 (Print)
© College of Natural Sciences, Addis Ababa University, 2016 2520–7997 (Online)

HYDRATION STRUCTURE AND WATER EXCHANGE DYNAMICS OF Na(I)ION IN AQUEOUS SOLUTION

Ahmed Mustefa Mohammed

Department of Chemistry, College of Natural and Computational Sciences, Addis Ababa University,
P. O. Box 1176, Addis Ababa, Ethiopia. Email: ahmed.mustefa@aau.edu.et

ABSTRACT: The hydration structure and water exchange dynamics in the first hydration shell for Na(I) in water are studied by molecular dynamics simulation. The structure of the hydrated ion is reported in terms of radial distribution functions, coordination numbers, and angular distributions. The average first-shell hydration structure is a 5.6, in agreement with experimental results. The classical umbrella-sampling molecular dynamic simulations was employed to investigate the water exchange reaction around the Na(I) ion in water. The water exchange mechanism proceeds via the I_d mechanism with the water exchange rate constant of 3.42×10^{11} s^{-1} at 298 K, estimated by the transition state theory assuming a transmission coefficient of unity.

Keywords/phrases: Hydration, Water exchange, Umbrella sampling, Molecular Dynamics, Sodium (I) ion

INTRODUCTION

Solvated ions appear in living organisms, where their presence or absence can fundamentally alter the functions of life and their solvation is one of the most fundamental chemical processes (Sigel, A. *et al.,* 2016; Mahler, J. and Persson, I., 2012). In many of these cases, understanding the selective solvation and the dynamics of the ions is essential for the understanding of the processes involved. Hence, great efforts have been done to determine the structure and dynamics of metal ions in solution by a variety of experimental techniques (Mahler, J. and Persson, I., 2012; Ohtaki, H. and Radnai, T., 1993; Marcus, Y., 2009; Cotton, F.A. *et al*., 1993; Helm, L. and Merbach, A. E., 2005; Mahler, J. and Persson, I., 2012; Ohtaki, H. and Radnai, T., 1993; Marcus, Y., 2009; Ozutsumi, K. *et al*., 1993; Cotton, F.A. *et al*., 1993; Helm, L. and Merbach, A. E., 2005; Marini, G.W. *et al*., 1999; Kowall, T. *et al*., 1995; Marx, D. *et al*., 1997; Kerdcharoen, T. *et al*., 1996; Martinez, J.M. *et al*., 2000; Inada, Y. *et al*., 2002; Ahmed M. Mohammed, 2006; Iglesias-Yagüe, J. *et al*., 2003; Loeffler, H.H. *et al*., 2003; Ahmed M. Mohammed, *et al*., 2005; Rode, B.M. and Islam, S.M., 1991; Yongyai, Y. *et al*., 1991; Rotzinger, F. P., 2005). Nevertheless, experimental investigations often yield an incomplete description of ionic solvation. Recently, simulations techniques have emerged as successful complement to experimental techniques and have led to a greater understanding of solvation processes.

Sodium(I) being one of those ions that appear in living organisms plays a diverse and important role in many physiological processes such as the signal transduction in the human central nervous system Hence, the hydration structure of sodium ion has been the subject of many experimental and theoretical investigations, (White, J. A. *et al*., 2000; Kameda, Y. *et al*., 1998; Koneshan, S. *et al*., 1998; Tongraar, A. *et al*., 1998; Toth, G., 1996; Obst S. and Bradaczek, H., 1996; Degrève, L. and da Silva, F., 1999; Sikander Azam, S. *et al*., 2009; Lev, B. B. *et al*., 2010; Xu, J. *et al*., 2009; Kerisit, S. and Rosso, K. M., 2009; Inada, Y. *et al*., 2002). However, the dynamics especially the ligand substitution around the ion has been less studied due to limitation in both experimental and theoretical methods (Helm, L. and Merbach, A. E., 2005; Rotzinger, F. P., 2005).

Simulation techniques such as molecular dynamics (MD) provide molecular levels of detail of the hydration processes that are usually difficult to determine by experimental techniques. MD techniques using a pair potential supplemented by three-body potentials obtained from *ab initio* calculations have been used widely to study hydration structures of metal and in many cases have reproduced properly the hydration structures (Kowall, T. *et al*., 1995; Marx, D. *et al*., 1997; Kerdcharoen, T. *et al*., 1996; Martinez, J.M. *et al*., 2000; Inada, Y. *et* *al*., 2002; Ahmed M. Mohammed, 2006; Iglesias-Yagüe, J. *et al*., 2003; Loeffler, H.H. *et al*., 2003; Ahmed M. Mohammed, *et al*., 2005; Rode, B.M. and Islam, S.M., 1991; Yongyai, Y. *et al*., 1991). Furthermore, simulation techniques have been playing vital role in providing insight into water exchange processes around hydrated metal ions (Inada, Y. *et al*., 2002; Schwenk, C.F. *et al*., 2001; Hermansson and K.; Wojcik, M., 1998; Inada, Y *et al*., 2005; Loeffler, H.H. *et al*., 2006; Ahmed M. Mohammed, 2008;. Ahmed M. Mohammed, 2010). Water exchange processes of many metal ions often occur on timescales larger than the nanosecond range typical for standard MD simulations (Helm, L. and Merbach, A. E., 2005). Therefore, observing the transition state (TS) is quite rare during a simulation leading to unreliable results. In order to increase the probability of finding high energy states and hence enhancing sampling efficiency in a specific region of phase space a biasing function driving particles along a chosen reaction coordinate may be applied. One powerful approach to adequately sample high energy, i.e. a transition state, is the umbrella-sampling technique (Valleau, J.P. and Torrie, G.M., 1977), which has been widely used to calculate reaction profiles for chemical processes in solution (Inada, Y *et al*., 2005; Loeffler, H.H. *et al*., 2006; Ahmed M. Mohammed, 2008;. Ahmed M. Mohammed, 2010; Kumar, S. *et al*., 1995; Boczko, E.M. and Brooks III, C.L., 1995; Boczko, E.M. and Brooks III, C.L., 1993; Kumar, S. *et al*., 1992;Roux, B., 1995). It has been successfully applied to study water exchange processes around other first row-transition metal ions in water (Schwenk, C.F. *et al*., 2001; Hermansson K. and Wojcik, M., 1998; Inada, Y *et al*., 2005; Loeffler, H.H. *et al*., 2006; Ahmed M. Mohammed, 2008;. Ahmed M. Mohammed, 2010).

In this study, 2-body (2bd) potential for Na(I)–H_2O interaction and its 3-body (3bd) correction terms (H_2O –Na(I)– H_2O) were evaluated by means of *ab initio* molecular orbital calculations and corresponding analytical functions were constructed. Standard MD simulation was carried out for Na(I)in water using the 2-body potential and its 3-body correction function to study hydration structure of the Na(I)ion. Furthermore, the present study investigates the water exchange processes around the Na(I)ion in the aqueous solution. Emphasis is given on the enlightenment of the structural changes at the transition state during the replacement of a water molecule from the first shell by a water molecule from the second hydration shell. Free energy profile along the chosen reaction coordinate was determined and used to obtain the exchange mechanism and reaction rate of the water exchange process. In order to do sampling along a reaction coordinate umbrella-sampling technique was applied. The water exchange reaction is determined from the viewpoint of a dissociative unimolecular approach (S_N1 in terms of standard organic chemistry nomenclature).

COMPUTATIONAL DETAILS

Construction of ion-water pair potential

The pair-potential for the Na(I) water interaction was newly constructed by *Ab initio* molecular orbital calculations at the restricted Hartree-Fock (RHF) level using the Gaussian 98 program (Frisch, M.J. *et al.* 2001). The experimental gas-phase geometry of H_2O was used with the O–H distance of 0.9601 Å and the H–O–H angle of 104.47° (Kuchitsu, K. and Morino, Y., 1965).

To calculate the 2-body interaction energies between Na(I)and H_2O, the position of the Na(I)ion was varied around the H_2O molecule by fixing the O atom at the origin, two H atoms on the xz plane, and the C_{2v} axis of H_2O on the z axis of the Cartesian coordinate system. The values of the Na(I) –O distance (r_{NaO}), the angle between the O–Na vector and the z axis (θ), and the angle between the x axis and the projection of the O–Na vector onto the xy plane (ϕ) were varied over the ranges 1.5 Å $\leq r_{\mathrm{NaO}} \leq$ 15.0 Å, 0° $\leq \theta \leq$ 180°, and 0° $\leq \phi \leq$ 90°, respectively. The 2-bodyinteraction energies (E_{2bd}) were calculated by subtracting the SCF energies (E_{Na} and E_{W}) of isolated Na(I)and H_2O from that (E_{NaW}) of $[\mathrm{Na(H_2O)}]^{2+}$, as expressed by Eq. 1.

$$E_{\mathrm{2bd}} = E_{\mathrm{NaW}} - E_{\mathrm{Na}} + E_{\mathrm{W}} \qquad (1)$$

To represent the E_{2bd} values by an analytical function, various functions were tested to fit to the E_{2bd} values by a least-squares optimization using the Levenberg-Marquardt algorithm. The best reproducibility was obtained using a function composed of four *r-m* terms for the non-Coulombic interaction in addition to the Coulombic interaction, as expressed by Eq. 2,

$$E_{2bd} = \frac{Q_{Na}Q_{O}}{r_{NaO}} + A_{O}r_{NaO}^{-5} + B_{O}r_{NaO}^{-6} + C_{O}r_{NaO}^{-9} + D_{O}r_{NaO}^{-11} + \sum_{i=1}^{2}\left(\frac{Q_{Na}Q_{H_i}}{r_{NaH_i}} + A_{H}r_{NaH_i}^{-5} + B_{H}r_{NaH_i}^{-6} + C_{H}r_{NaH_i}^{-9} + D_{H}r_{NaH_i}^{-11}\right) \quad (2)$$

where Q is the atomic net charge, r_{NaH} is the distance between Na and H, and A, B, C, and D are optimization parameters. The values of -0.6596 and 0.3298 were adopted for Q_O and Q_H, respectively, from the central-force (CF) model for H_2O (Lemberg, H.L. and Stillinger, F.H., 1975).

The value of Q_{Na} was assumed to be 1. E_{2bd} values near the global energy minimum were emphasized during the least-squares procedure by assigning an appropriate weighting factor. E_{2bd} values above 30 kcal mol^{-1} were excluded in the optimization of the function. The optimized potential parameters are given in Table 1.

Construction of 3-body correction term

The 3-body correction energy (E_{3bd}) was calculated according to Eq. 3,

$$E_{3bd} = E_{NaW_iW_j} - (E_{Na} + 2E_{W}) - (E_{NaW_i} + E_{NaW_j}) - E_{W_iW_j} \quad (3)$$

where $E_{NaW_iW_j}$ is the SCF energy for $[Na(H_2O)_2]^{2+}$, E_{NaW_i} and E_{NaW_j} are the 2-body interaction energies, calculated using the previously developed analytical function (Eq. 2), and $E_{W_iW_j}$ is the intermolecular potential between H_2O molecules computed using the CF2 model (Stillinger, F.H. and Rahman, A., 1978). The SCF–energy calculations were performed by varying independently both Na–O distance ($2.0 \le r_{NaO} \le 6.0$ Å) and the O–Na–O angle ($60° \le \psi \le 180°$). The dipole moments of both H_2O molecules were fixed to point toward the Na(I)ion for all configurations. Almost all of the E_{3bd} values were found to be positive for the geometries employed in this study. The E_{3bd} value decreases with increasing r_{NaO} and becomes almost 0 kcal mol^{-1}when either r_{NaO} approaches to 6.0 Å. Furthermore, given a set of two r_{NaO} distances, the E_{3bd} value fell off with increasing distance between the two H_2O molecules. The E_{3bd} function can be expressed by Eq. 4,

$$E_{3bd} = F\exp[-G(r_{NaO_i} + r_{NaO_j})] \times \exp(-Hr_{ij})[(R_{CL} - r_{NaO_i})^2 \times (R_{CL} - r_{NaO_j})^2] \quad (4)$$

where F, G, and H are fitting parameters, r_{ij} is the distance between two oxygen atoms of H_2Omolecules, and R_{CL} is the cutoff limit of 6.0 Å for the 3-body correction function. The final term in Eq. 4 guarantees that E_{3bd} vanishes if r_{NaO_i} or r_{NaO_j} become larger than R_{CL}. The analytical function of Eq. 4 was fitted to the E_{3bd} values by a least-squares optimization, and the final parameters are given in Table 1.

Table 1. Parameters for two-body potential and three-body correction function of Na(I)−water interactions.

		2−body			
	Atom	A (kcal/mol)$^{-A}$	B (kcal/mol)$^{-B}$	C (kcal/mol)$^{-C}$	D (kcal/mol)$^{-D}$
Na	O	−5910.55	13496.52	−14990.26	6388.37
	H	1793.53	-4084.27	9261.25	-8649.95
		3−body			
		F (kcal/mol Å^{-4})		G(Å^{-1})	H(Å^{-1})
H_2O−Na(II)−H_2O		0.2100544		0.5518802	0.0772374

Standard MD simulation

The standard MD simulation method applied in this study was described in detail in previous paper (Ahmed M. Mohammed, 2005). and will only be briefly reviewed here. The simulation system consisting of one Na(I) ion and 499 water molecules in a cubic simulation box of 15010.9 Å^3 subjected to periodic boundary conditions. The simulations were performed in the *NVT* ensemble with a time step of 0.2 fs. The density of the simulation box was set to the experimental value of pure water at 298.16 K (0.997 g cm^{-3}). Long range interactions were treated by the reaction field method (Allen, M. P.

and Tildesley, D. J. 1987). The CF2 model was used for the intermolecular potential between H_2O molecules, and the intramolecular potential of H_2O developed by Bopp *et al*. was employed to reproduce correctly liquid-phase vibrational frequencies (Bopp, P. *et al*., 1983). In order to construct the initial configuration, the O atoms of H_2O were placed in the simulation box according to the face-centered cubic lattice. The H atoms were arranged with random configuration of H_2O molecules. A total of 400,000 steps (80 ps) were first processed using only the 2-body potential, and the system was confirmed to be energetically equilibrated. A further 400,000 steps (80 ps) were sampled to evaluate structural properties. The simulation was continued for further 400,000 steps (80 ps) of equilibrium after the inclusion of the 3-body correction. All energies were confirmed to become stable within 5 ps of equilibrium. A further 1,000,000 steps (0.2 ns) simulation was carried out for the statistical sampling.

Umbrella-sampling MD simulations

A randomly chosen water molecule from the first hydration shell was moved to the second hydration under the influence of the umbrella potential V_{umb}:

$$V_{\text{umb}}(r_o) = \frac{k}{2}(r_{ob} - r_o)^2 \qquad (5)$$

where r_o is the instantaneous Na–O distance between Na(I)and a dissociating water molecule. The parameter k denotes the force constant and r_{ob} is the restrained Na–O distance. The distance r_o was varied between 2.40 Å and 3.8 Å to cover the full range between first and second hydration shells. The force constant k was adjusted according to r_o, i.e. k was set to high values close to the transition state and to small values at minima in the PMF. The unbiased probability distribution <r(r_o)> was obtained by the WHAM method to calculate the PMF according to Eq. 6

$$W(r_o) = -k_{\text{B}}T \ln\langle \rho(r_o)\rangle + C \qquad (6)$$

where k_{B} is the *Boltzmann constant*, T the absolute temperature, and C an arbitrary constant. An estimate for the reaction rate constant k_{ex} may then be determined from the free energy difference $\Delta G^{\ddagger}$ between the ground and transition state via the classical *Eyring equation* (Eq. 7)

$$k_{\text{ex}} = \kappa \frac{k_B T}{h} \exp\left(-\frac{\Delta^{\ddagger} G}{\text{RT}}\right) \qquad (7)$$

where k is the transmission coefficient, k_{B} is the *Boltzmann constant*, h is the *Planck constant*, R is the gas constant, and T is the *absolute temperature*.

The simulation protocol was the same as in the standard MD simulation. The starting configuration of the system was taken from the last configuration of the standard simulation obtained using the corrected 2-body potential. In total, 15 independent MD simulations were carried out with 200 ps each reserved for data collection after the system was allowed to reach the equilibrium within 2 ps. Several test simulations have been performed to ensure the independence of the chosen parameters.

RESULTS AND DISCUSSION

Structural properties

The Na(I)–O and Na(I)–H radial distribution functions (RDFs), and their running integration numbers obtained from the standard MD simulation are displayed in Figure 1. The main structural parameters are listed and compared with experimental and other simulation investigations in Table 2. The first peak of the Na(I)–O RDF which is associated to the first hydration shell reaches its maximum at 2.41 Å, the experimental mean Na(I)–O distance varies from 2.40 to 2.50 Å (Ohtaki, H. and Radnai, T., 1993). The second peak related to the second hydration shell reaches its maximum at 4.73 Å, undoubtedly separated from the first hydration sphere. The Na(I)−O RDF between the first and second shells doesn't go zero suggesting that the first shell and the second could easily interchange water molecules.

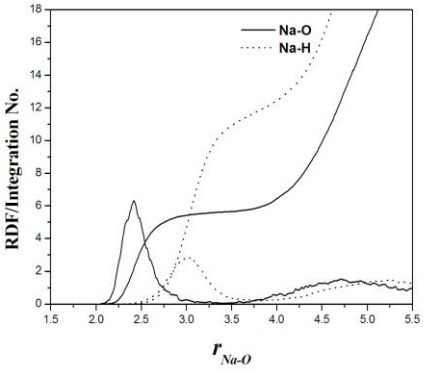

Figure 1. Na(I)−O and Na(I)−H radial distribution functions and their running integration numbers obtained by the standard MD simulation.

Table 2. Hydration structure parameters of the Na(I)ion in water determined by standard molecular simulations and experimental methods.

System	r_{max}	g_{max}	r_{min}	g_{min}	n_c	Method	Ref.
NaI	2.43	-	-	-	6.0	LXAS	2
Na$^+$	2.49	3.6	3.2	0.5	5.2	MD (QM)	21
NaCl	2.39	-	-	-	4.6	x ray	22
NaClO$_4$	2.39	-	-	-	4	x ray	22
Na$^+$	2.45	7.21	3.25	0.16	5.8	MD (SPC/E)	23
Na$_2$SO$_4$	2.35	-	-	-	6.0	x ray	30
Na$^+$	2.33	5.5	2.9	0.5	5.6	MD(QM/MM)	24
Na$^+$	2.36	-	-	-	6.5	MD(CF2)	34
Na$^+$	2.43	5.5	3.2	0.7	7.3	MD(TIP4P)	25
Na$^+$	2.47	6.7	3.2	0.2	6.0	MD(TIP3P)	26
NaCl	2.29	9.0	3.1	0.1	5.8	MC(TIP4P)	27
Na$^+$	2.36	-	3.45	-	5.5	QM/MM MD	28
Na$^+$	2.34	-	3.46	-	5.5	QMCF MD	28
Na$^+$	2.325	4.425	3.125	-	5.68	MD(SPC/E)	31
Na$^+$	2.41	4.8	3.5	0.1	5.6	MD(CF2)	This work

The presence of two hydration shells is also clearly shown in the Na(I)−H RDF (Figure 1). The first peak is centered at 2.96 Å and the second at 5.18 Å. The shift of the peaks in Na(I)−HRDF to larger distances with respect to the corresponding oxygen peaks indicates that especially in the first shell, the water molecules are well oriented to obey the dominant ion−water interactions with their oxygen atoms pointing to the ion.

The coordination number distribution (CND) probability obtained by the standard MD simulation is shown in Figure 2. The average coordination number (CN) in the first coordination sphere which is obtained by integrating the RDF up to the first minimum is 5.6. This value is in very good agreement with QM/MM results (Tongraar, A. *et al.*, 1998) and is within the range of the reported experimental data (Table 2, Ref. 3). The second coordination sphere hydration shell contains on average 16.8 water molecules, implying that every first shell water molecule interacts with about 3 water molecules. This reveals that ligand orientation and binding is not entirely determined by hydrogen bonding.

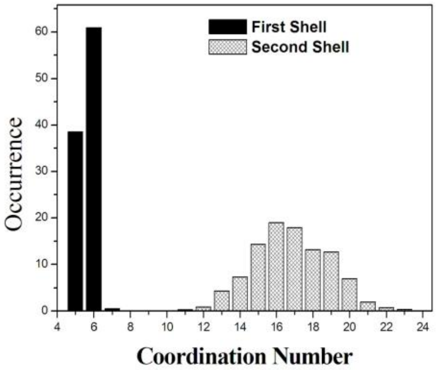

Figure 2. First and second shell coordination number distribution of hydrated Na(I)obtained by the standard MD simulation.

The probability of finding O–Na–O angle (*θ*) in the first hydration shell, the first-shell angular distribution function (ADF), obtained from the standard simulation is shown in Figure 3 as a function of 1-*cosθ*. Two well-defined peaks can be observed at the peak maxima of 90° and180°.

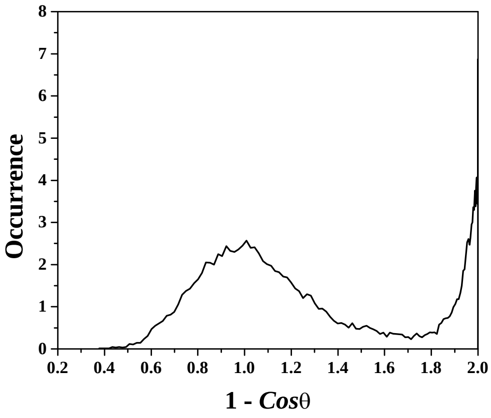

Figure 3. First-shell angular distribution functions for O–Na–O (θ) in the first hydration shell of the Na(I)ion as a function of 1-*Cos*θ obtained by the standard MD simulation.

Potential of mean force (PMF) and rate constant

The PMF has characteristic shape with a first minimum at 2.48 Å that corresponds to the average Na(I)–O distance for the first hydration shell (Figure 4). The second minimum describes a recovered hydration in the first shell; however, at this point the dissociating water molecule has left the first shell and replaced by a water molecule from the second shell.

The PMF maxima corresponding to the transition state of the water-exchange process is located at 3.43 Å. The free energy of activation ($\Delta G^{\ddagger}$), the energy difference between the ground state (first PMF minimum) and the transition state (first PMF maximum), is 7.19 kJ/mol (1.72 kcal/mol). According to the transition-state theory (Eq. 7), the water exchange rate constant k_{ex} for Na(I) ion at 298.16 K is 3.42 x 10^{11} s^{-1}, assuming a transmission coefficient, *k,* to be unity. This value, considering the uncertainty of *k* and the simplicity of the potential functions used in this study, is quite reasonable (Helm, L. and Merbach, A. E., 2005).

Furthermore, the absence of an intermediate in the PMF (Figure 4) suggests that the water exchange process is taking place via the interchange (I) mode of the mechanism. The running integration number of Na(I) close to the transition state has a hydration number about 5 (excluding the dissociating water molecule) at the distance of the transition state of 3.43 Å. This indicates that the number of water molecules in the first hydration shell at the transition state is less than in the ground state, suggesting the dissociative mode of the activation.

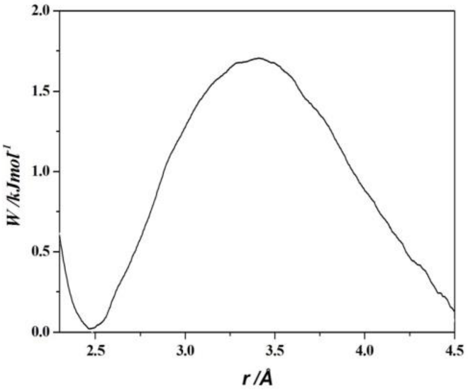

Figure 4. Potential of mean force (PMF) for water exchange process of around Na(I)ion.

The water exchange reaction around Na(I) ion, therefore, proceeds *via* an I_d mechanism in agreement with the experimental observation (Rotzinger, F. P., (2005).

CONCLUSIONS

The first shell coordination numbers and ion-ligand distances obtained with the standard MD simulation including 3-body effects are in good agreement with the experimental data. Based on the structural analysis of the first shell at the transition state, water exchange reaction around Na(I) ion proceeds via I_d mechanism in agreement with experimental observations. The water exchange rate constant is relatively high (3.42 x 10^{11} s^{-1}) but it is reasonable given the unknown transmission coefficient and the assumptions made in constructing the Na(I)-water potential functions. In general, these results demonstrate that the umbrella-sampling MD simulation is a reliable tool to study ligand exchange processes around metal ions, not only where experimental investigation is impossible or difficult, but also in processes which cannot be studied by standard MD simulations.

AKNOWLEDGEMENTS

The author is grateful to the Department of Chemistry, Addis Ababa University for the computational facilities.

REFERENCES

1. Ahmed M. Mohammed (2006). Structure of Co(III) and Fe(III) transition metal ions in aqueous solution. *Bull. Chem. Soc. Ethiop*. 20, 121-131.
2. Ahmed M. Mohammed (2008). Hydration of Cd(II): Molecular dynamics study. *Bull. Chem. Soc. Ethiop*., **22**, 423-432.
3. Ahmed M. Mohammed (2010). Hydration structure and water exchange dynamics of Fe(II) ion in aqueous solution. *Bull. Chem. Soc. Ethiop*. **24(2),** 239-250.
4. Ahmed M. Mohammed; Loeffler, H.H.; Inada, Y.; Funahashi, S. (2005). Quantum mechanical/ molecular mechanical molecular dynamic simulation of zinc(II) ion in water. *J. Mol. Liq*. ***119***, 55-62.
5. Allen, M. P.; Tildesley, D. J. (1987). *Computer Simulation of Liquids*; Clarendon Press: Oxford, U.K.
6. Bopp, P.; Jancsó, G.; Heinzinger (1983). An improved potential for non-rigid water molecules in the liquid phase. K. *Chem. Phys. Lett*., **98**, 129-133.
7. Boczko, E.M.; Brooks III, C.L. (1995). First-principles calculation of the folding free energy of a three-helix bundle protein. *Science*, **269**, 393-396.
8. Boczko, E.M. Brooks III, C.L. (1993). Constant-temperature free energy surfaces for physical and chemical processes. *J. Phys. Chem.* **97**, 4509-4513.
9. Cotton, F.A.; Daniels, L.M.; Murillo, C.A.; Quesada, J.F. (1993). Hexaaqua dipositive ions of the first transition series: new and accurate structures; expected and unexpected trends. *Inorg. Chem.* 32, 4861-4861.
10. Degrève, L.; da Silva, F. (1993). Structure of concentrated aqueous NaCl solution: A Monte Carlo study. *J. Chem. Phys.* **110,** 3070-3078.
11. Frisch, M.J.; Trucks, G.W.; Schlegel, H.B.; Scuseria, G.E.; Robb, M.A.; Cheeseman, J.R.; Zakrzewski, V.G.; Montgomery, J.A.Jr.; Stratmann, R.E.; Burant J.C.; Dapprich, S.; Millam, J.M.; Daniels, A.D.; Kudin, K.N.; Strain, M.C.; Farkas, O.; Tomasi, J.; Barone, V.; Cossi, M.; Cammi, R.; Mennucci, B.; Pomelli, C.; Adamo, C.; Clifford, S.; Ochterski, J.; Petersson, G.A.; Ayala, P.Y.; Cui, Q.; Morokuma, K.; Salvador, P.; Dannenberg, J.J.; Malick, D.K.; Rabuck, A.D.; Raghavachari, K.; Foresman, J.B.; Cioslowski, J.; Ortiz, J.V.; Baboul, A.G.; Stefanov, B.B.; Liu, G.; Liashenko, A.; Piskorz, P.; Komaromi, I.; Gomperts, R.; Martin, R.L.; Fox, D.J.; Keith, T.; Al-Laham, M.A.; Peng, C.Y.; Nanayakkara, A.; Challacombe, M.; Gill, P.M.W.; Johnson, B.; Chen, W.; Wong, M.W.; Andres, J.L.; Gonzalez, C.; Head-Gordon, M.; Replogle, E. S and Pople, J.A. (2001) *Gaussian 98 Revision A.11,* Gaussian: Pittsburgh PA.
12. Helm, L.; Merbach, A. E. (2005). Inorganic and bioinorganic solvent exchange mechanisms. *Chem. Rev.* **105**, 1923-1959.
13. Hermansson, K.; Wojcik, M. (1998). Water Exchange around Li^+ and Na^+ in LiCl(aq) and NaCl(aq) from MD Simulations. *J. Phys. Chem. B* **102**, 6089-6097.
14. Iglesias-Yagüe, J.; Ahmed M. Mohammed; Loeffler, H.H.; Rode, B.M. (2003). MD and MC simulations of hydrated manganous ion including three-body effects. *J. Mol. Struct.: Theochem* , **620**, 15-20.
15. Inada, Y.; Loeffler, H.H.; Rode, B.M. (2002). Librational, vibrational, and exchange motions of water molecules in aqueous Ni(II) solution: classical and QM/MM molecular dynamics simulations. *Chem. Phys. Lett.* , **358**, 449-458.
16. Inada, Y.; Ahmed M. Mohammed; Rode, B.M. Loeffler, H. (2002). Hydration Structure and Water Exchange Reaction of Nickel(II) Ion: Classical and QM/MM Simulations. *J. Phys. Chem. A*., **106**, 6783 6783-6791.
17. Inada, Y.; Ahmed M. Mohammed; Loeffler, H.H. Funahashi, S. (2005). Water-exchange mechanism for zinc(II), cadmium(II), and mercury (II) ions in water as studied by umbrella-sampling molecular-dynamics. *Helv. Chim. Acta* , **88**, 461-469.
18. Kameda, Y.; Sugawara, K.; Usuki, T.; Uemura, O. (1998). Hydration Structure of Na^+ in Concentrated Aqueous Solutions. *Bull. Chem. Soc. Jpn*., **71**, 2769-2776.
19. Kerdcharoen, T.; Liedl, K.R.; Rode, B.M. (1996). A QM/MM simulation method applied to the solution of Li^+ in liquid ammonia. *Chem. Phys*., **211**, 313-323.
20. Kerisit, S.; Rosso, K. M. (2009). Transition path sampling of water exchange rates and mechanisms around aqueous ions. *J. Chem. Phys*., **131**, 114512-114526.
21. Koneshan, S.; Rasaiah, J. C.; Lynden-Bell, R. M.; Lee, S. H. (1998). Solvent Structure, Dynamics, and Ion Mobility in Aqueous Solutions at 25°C. *J. Phys. Chem. B,* **102** (21), 4193-4204.
22. Kowall, T.; Foglia, F.; Helm, L.; Merbach, A.E. (1995). Molecular Dynamics Simulation Study of Lanthanide Ions Ln^{3+} in Aqueous Solution Including Water Polarization. Change in Coordination Number from 9 to 8 along the Series. *J. Am. Chem. Soc.* , **117**, 3790-3799.
23. Kuchitsu, K.; Morino, Y. (1965). Estimation of anharmonic potential constants. II. Bent XY_2 molecule. *Bull. Chem. Soc. Jpn*. **38**, 814-824.

24. Kumar, S.; Bouzida, J. D.; Swendsen, R. H.; Kollman, P.A.; Rosenberg, J.M. (1992). The weighted histogram analysis method for free-energy calculations on biomolecules. I. The method. *J. Comput. Chem.*, **13,** 1011-1021.
25. Kumar, S.; Rosenberg, J.M.; Bouzida, J.D.; Swendsen, R.H.; Kollman, P.A. (1995). Multidimensional free-energy calculations using the weighted histogram analysis method. *J. Comput. Chem.*, **16**, 1339-1350.
26. Lemberg, H.L.; Stillinger, F.H. (1975). Central-force model for liquid water. *J. Chem. Phys.*, **62**, 1677-1690.
27. Lev, B.B.; Salahub, D.R.; Noskov, S.Y. (2010). Na^+, K^+ and Tl^+ hydration from QM/MM computations and MD simulations with a polarizable force field. *Interdiscip Sci Comput Life Sci.***,** 2, 12-20.
28. Loeffler, H.H.; Ahmed M. Mohammed; Inada, Y.; Funahashi, S. (2003). Lithium(I) ion hydration: a QM/MM-MD study. *Chem. Phys. Lett.*, 379,452-457.
29. Loeffler, H.H.; Ahmed M. Mohammed; Inada, Y.; Funahashi, S. (2006). Water exchange dynamics of Mn^{2+}, Co^{2+}, and Ni^{2+} ions in aqueous solution. *J. Comp. Chem.*, 27, 1944-1949.
30. Mahler J.; Persson, I. (2012). A Study of the Hydration of the Alkali Metal Ions in Aqueous Solution. *Inorg. Chem.* 51, 425-438.
31. Marcus, Y. Effect of ions on the structure of water: structure making and breaking. *Chem. Rev.*, **2009**, 109 (3), 1346-1370.
32. Marini, G.W.; Liedl, K.R.; Rode, B.M. (1999). Investigation of Cu^{2+} Hydration and the Jahn−Teller Effect in Solution by QM/MM Monte Carlo Simulations. *J. Phys. Chem. A*, **103**, 11387-11393.
33. Martinez, J.M.; Hernandez-Cobos, J.; Saint-Martin, H.; Pappalardo, R.R.; Ortega-Blake, I.; Sánchez-Marcos, E. *(2000).* Coupling a polarizable water model to the hydrated ion-water interaction potential: A test on the Cr^{3+} hydration. *J. Chem. Phys.*, **112(5)**, 2339-2347.
34. Marx, D.; Sprik, M.; Parrinello, M. (1997). Ab initio molecular dynamics of ion solvation. The case of Be^{2+} in water. *Chem. Phys. Lett.*, **273**, 360-366.
35. Obst S.; Bradaczek, H. (1996). Molecular dynamics study of the structure and dynamics of the hydration shell of alkaline and alkaline-earth metal cations. *J. Phys. Chem.* **100**, 15677-15687.
36. Ohtaki, H.; Radnai, T. (1993). Structure and Dynamics of Hydrated Ions. *Chem. Rev.*, **93**, 1157-1204.
37. Ozutsumi, K.; Koide, M.; Suzuki, H.; Ishiguro, S. (1993). Solvation structure of divalent transition-metal ions in N,N-dimethylformamdie and N,N-dimethylacetamdie. *J. Phys. Chem.*, **97(2),** 500-502.
38. Rode, B.M.; Islam, S.M. (1991). Monte Carlo Simulations with an Improved Potential Function for Cu(II)-Water Including Neighbour Ligand Corrections *Z. Naturforsch Teil A* , **46**, 357-362.
39. Rotzinger, F. P. (2005). Treatment of substation and rearrangement mechanisms of transition metal complexes with quantum chemical methods. *Chem. Rev.*, **105**, 2003-2037.
40. Roux, B. (1995). The calculation of the potential of mean force using computer simulations. *Comput. Phys. Commun.*, **91**, 275-282.
41. Schwenk, C.F.; Loeffler, H.H.; Rode, B.M. (2001). Dynamics of the solvation process of Ca^{2+} in water. *Chem. Phys. Lett.*, **349**, 99-103.
42. Sigel, A., Sigel, H.; Sigel, R. K. O. (Eds.) (2016). *The Alkali Metal Ions: Their Role for Life*, Springer International Publishing.
43. Sikander Azam, S.; Hofer, T.S.; Randolf, B.R.; Rode, B.M. (2009). Hydration of sodium(I) and potassium(I) revisited: A Comparative QM/MM and QMCF MD simulation study of weakly hydrated Ions. *J. Phys. Chem. A*, **113**, 1827-1834.
44. Stillinger, F.H.; Rahman, A. (1978). Revised central force potentials for water. *J. Chem. Phys.*, **68**, 666-670.
45. Tongraar, A.; Liedl, K. R.; Rode, B. M. (1998). Born−Oppenheimer ab Initio QM/MM Dynamics Simulations of Na^+ and K^+ in Water: From Structure Making to Structure Breaking Effects. *J. Phys. Chem. A*, **102**, 10340-10347.
46. Toth, G. (1996). *Ab initio* pair potential parameter set for the interaction of a rigid and a flexible water model and the complete series of the halides and alkali cations. *J. Chem. Phys.*, **105**, 5518-5524.
47. Valleau, J.P.; Torrie, G.M. (1977). *Statistical Mechanics, Part A: A Guide for Monte Carlo for Statistical Mechanics*, Berne, B.J. (Ed.), Plennum: New York.
48. White, J. A.; Schwegler, E.; Galli, G.; Gygi, F. (2000). The solvation of Na^+ in water: First-principles simulations. *J. Chem. Phys.*, **113(11),** 4668-4673.
49. Xu, J.; Fang, Y.; Fang, C. (2009). Structure of aqueous sodium sulfate solutions derived from X-ray diffraction. *Chinese Sci Bull*, **54**, 2022-2027.
50. Yongyai, Y.; Kokpol, S.; Rode, B.M. (1991). Zinc ion in water: intermolecular potential with approximate three-body correction and Monte Carlo simulation. *Chem. Phys.*, **156**, 403-412.